Photocatalytic degradation of acetone and butane on mesoporous titania layers

Václav Štengl,* Vendula Houšková, Snejana Bakardjieva and Nataliya Murafa

Received (in Montpellier, France) 3rd March 2010, Accepted 13th April 2010
DOI: 10.1039/c0nj00167h

Mesoporous titania was prepared by homogeneous hydrolysis of titanium oxo-sulfate with urea in aqueous solutions in the presence of the cationic and anionic surfactants, cetyl trimethyl ammonium bromide (CTAB) and sodium dodecyl benzene sulfonate (SDBS), respectively. Following annealing at 600 °C the structure of prepared samples was determined with X-ray powder diffraction (XRD) and selected area electron diffraction (SAED). The morphology and microstructure characteristics were also obtained by scanning electron microscopy (SEM) and high resolution electron microscopy (HRTEM). Surface area (BET) and porosity were also determined. From the mesoporous titania samples, a 300 μm thin layer on glass desk 10 × 15 cm was created. The photocatalytic activity of the prepared layers was assessed from the kinetics of the photocatalytic degradation of butane and acetone in the gas phase.

1. Introduction

Mesoporous titania has attracted much attention, since its high surface-to-volume ratio offers potentially more active reaction sites, making it of great importance in, for example, photocatalysis and photoelectrical chemical conversion. TiO_2 samples with different anatase/rutile ratios were prepared by calcination at different temperatures from commercial photocatalyst Degussa P25. The effects of the two crystalline phases of titanium(IV) oxide on the photocatalytic activity in gaseous phase through oxidation of light hydrocarbons have been studied. Results indicate that samples with higher anatase/rutile ratios had higher intrinsic activities for the photodegradation of a propane/isobutane/butane (40:35:25 vol%) mixture.[1] Low molecular weight alkanes including propane, isobutane and n-butane can be completely oxidized to carbon dioxide and water vapor using a tubular photoreactor containing a supported ZrO_2–TiO_2 thin-film photocatalyst.[2] The kinetics of the total photocatalytic oxidation of alkanes on irradiated TiO_2 was investigated.[3] The dependence of reaction rate on starting concentrations, absorbed intensity, irradiation wavelength and temperature was also followed. Thin films of photocatalytic TiO_2 and ZnO were deposited in Vycor tubing by a simple and reproducible spray pyrolysis technique, and photocatalytic efficiency for butane degradation was compared to that of Degussa P-25 TiO_2 powder.[4]

Mesoporous titanium dioxide nanocrystalline powders were synthesized by ultrasonic-induced hydrolysis reaction of tetrabutyl titanate ($Ti(OC_4H_9)_4$) in pure water without using any templates or surfactants. It was found that the as-prepared products by the ultrasonic method were composed of anatase and brookite phases. The photocatalytic oxidation of mixture of formaldehyde and acetone of the samples prepared by ultrasonic method is higher than that of commercial Degussa P25 and the samples prepared by conventional hydrolysis method.[5] Photocatalytic oxidation of acetone and ethanol over nanocrystalline TiO_2 powder was studied under batch conditions using an UV illuminated DRIFTS chamber as a photoreactor.[6] Photocatalytic oxidation of organic compounds in gas phase appears to be a promising process for remediation of polluted air. In this work,[7] the photocatalytic degradation of acetone, which is a typical pollutant of indoor air, was investigated by using an annular photoreactor. A preliminary optical fiber reactor (OFR) that employs bare quartz fibers as a light-transmitting support of TiO_2 was tested for gas treatment by investigating photocatalytic oxidation of acetone in air (50–750 ppm). Using one or four TiO_2-coated fibers in a continuous flow photoreactor, a steady-state conversion up to 80% was achieved at ambient temperature and pressure.[8]

Photocatalytic oxidation of two ketones, acetone, and 2-butanone, over TiO_2-containing paper was studied under two different levels of relative humidity. Adsorption of these ketones on TiO_2-containing paper is significantly affected by the presence of water vapor.[9] Photocatalyzed degradations of trace levels of various oxygenates and an aromatic in air were carried out using near-UV-illuminated titanium dioxide (anatase) powder. The initial rates of degradation for acetone, 1-butanol, formaldehyde, and *m*-xylene were well described by Langmuir–Hinshelwood rate forms. No reaction intermediates were detected for acetone oxidation at conversions of 5–20%.[10] The effects of mixing condition by baffles, inlet concentration and face velocity on the photocatalytic degradation of gaseous acetone over thin-film TiO_2 have been examined in a continuous-flow system. Baffles enable the reactants to contact effectively the photocatalyst surface, and thus the rate can be increased.[11] Solid solutions of $Ti_{1-x}Zr_xO_2$ ($0.00 < x < 0.10$) exhibit higher photocatalytic activity than pure anatase TiO_2 for the degradation of acetone in air. The activity increases with increase of zirconium substitution in the TiO_2 lattice until nominal $x = 0.075$.[12] Solid solutions of $Ti_{1-x}V_xO_2$ ($0.00 < x < 0.025$) exhibit higher photocatalytic activity than pure TiO_2 for the oxidation of acetone, and the photocatalytic activity of the

Institute of Inorganic Chemistry v.v.i. Academy of Sciences of Czech Republic, Husinec-Rez 250 68, Czech Republic.
E-mail: stengl@iic.cas.cz

solid solution increases with increasing V substitution, but decreases with a decrease in the anatase to rutile ratio. The optimum composition in terms of activity is $x = 0.015$, with an anatase to rutile ratio of 9:1.[13] Photoactive films consisting of pure anatase, brookite or rutile TiO_2 were prepared by dip-coating from water dispersions obtained by using $TiCl_4$ as the precursor under similar mild experimental conditions, and the photoactivity of the films was determined employing the photo-degradation of 2-propanol.[14,15]

In the present work, the role played by the interactions between the simple cationic (CTAB) and anionic surfactant (SDBS) respectively and the TiO_2 surface during homogeneous hydrolysis growth step are investigated. The relative photocatalytic activities of the prepared thin layers of titania in poly(hydroxyethyl methacrylate) was assessed by the photocatalytic decomposition of butane and acetone, respectively. It is hoped that this work will contribute towards industry applications in the disposal of pollutants.

2. Experimental

2.1 Preparation of samples

All chemical reagents used were obtained from commercial sources and used without further purification. $TiOSO_4$, cetyl trimethyl ammonium bromide (CTAB), sodium dodecyl benzenesulfonate (SDBS) and urea were supplied by Fluka, Munich, Germany.

The mesoporous titania was prepared by homogeneous hydrolysis of $TiOSO_4$ aqueous solutions in the presence of cetyl trimethyl ammonium bromide (CTAB) and sodium dodecyl benzene sulfonate (SDBS), respectively. Urea was used as the precipitation agent. In a typical preparation, 100 g $TiOSO_4$ was dissolved in 100 mL hot distilled water acidified with 10 ml 98% H_2SO_4. The transparent liquid was diluted into 4 L of distilled water, 10 g of CTAB (sample TiCTAB10) or SDBS (sample Ti_DCB10) were added and mixed with 300 g of urea. The reaction mixture was initially at a pH of 0.95. The mixture was heated to 100 °C with stirring and kept at this temperature for 9 h until pH 7.5 was reached and ammonia escaped from the solution. The precipitates formed were washed with distilled water with decantation, filtered and dried at temperature 105 °C in a drying oven. In order to remove residual surfactants the prepared samples were heated to 600 °C for one hour under dynamic vacuum, using a furnace controlled by the PID controller in the quartz tube (sample denoted as TiCTAB10_600 and TIDCB10_600) The temperature increase rate was 1 °C min^{-1}. After the heat treatment, the sample was allowed to cool to room temperature. The prepared mesoporous titania powders (2 g) were dispersed in a mixture of 10 ml poly(hydroxyethyl methacrylate) and 10 ml of ethanol. From this suspension, a 300 μm thin layer on glass desk 100 × 150 mm was created.

2.2 Characterisation methods

X-ray diffraction (XRD) patterns were obtained using a Siemens D5005 instrument using Cu-Kα radiation (40 kV, 30 mA) and a diffracted beam monochromator. Qualitative analysis was performed with the DiffracPlus Eva Application (Bruker ASX) using the JCPDS PDF-2 database.[16] For quantitative phase analysis, mean coherence length analysis, and structural refinement, Rietveld analysis with DiffracPlus Topas (Bruker ASX) and structural models taken from ICSD database[17] were used.

The surface area of samples out-gassed for 60 min at 150 °C was determined from nitrogen adsorption–desorption isotherms at liquid nitrogen temperature using a Coulter SA3100 instrument. The Langmuir BET method was used for surface area calculation,[18] while pore size distribution (pore diameter and volume) was determined by the BJH method.[19]

Transmission electron microscopy (TEM and HRTEM) micrographs were obtained by using two instruments, namely a Philips EM 201 at 80 kV and a JEOL JEM3010 at 300 kV (LaB6 cathode). A copper grid coated with an amorphous perforated carbon film was used to prepare samples for the TEM observation. A powdered sample was dispersed in ethanol and the suspension was treated in an ultrasonic bath for 10 min prior to analysis.

Scanning electron microscopy (SEM) studies were performed using a Philips XL30 CP microscope equipped with EDX (energy dispersive X-ray), Robinson, SE (secondary electron) and BSE (back-scattered electron) detectors. The sample was placed on an adhesive C slice and coated with a layer of Au–Pd alloy (10 nm thick).

Kinetics of the photocatalytic degradation of gases was measured by using a home-made stainless steel batch photoreactor (see Fig. 1) with a Narva black-light fluorescent lamp (wavelength 365 nm, input power 8 W, light intensity 6.3 mW cm^{-2}). The gas concentration was measured with the use of Quadrupole Mass Spectrometer JEOL JMS-Q100GC and gas chromatograph Agilent 6890N. A high-resolution gas chromatography column (19091P-QO4, J&W Scientific) was used. Samples were taken from the reactor automatically through the sampling valve (6-port external volume sample injector VICI, Valco Instruments Co. Inc.) in a time interval of 30 min.

3. Results and discussion

It is well known[20,21] that homogeneous hydrolysis of metal salts with urea leads to spherical crystalline particles of the corresponding metal oxides. For example, hydrolysis of $TiOSO_4$ with urea[22] results in stable spherical TiO_2 microporous particles 1–2 μm in size being formed. For these solids, minimization of the surface energy leads to sphericity (see Fig. 2a). The final particle shape depends on whether oriented or isotropic aggregation takes place. Among the various factors that control the aggregation, dispersive forces and electrostatic inter-particle interactions are the most important. Oriented aggregation is a consequence of the dissimilar electrostatic charges that develop on the different crystal faces of the primary particles, which aggregate in the directions of minimum repulsion; this phenomenon occurs mainly when the overall particle charge is large. On the other hand, isotropic aggregation, which usually leads to the formation of spherical particles, takes place in the vicinity of the isoelectric point. The presence of the surfactants changes the surface energy and prevents formation of the spherical particles.

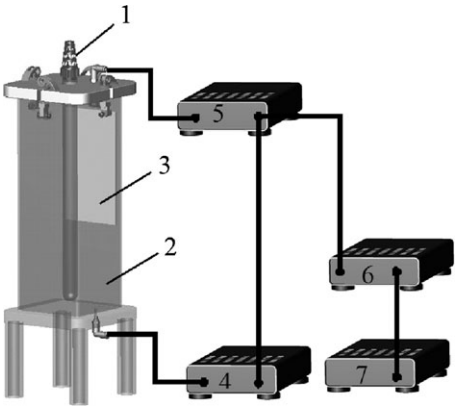

Fig. 1 (1) Fluorescent lamp, (2) stainless steel reactor, (3) glass desk with photocatalytic layer, (4) membrane pump, (5) sampling valve, (6) gas chromatograph, (7) mass spectrometer.

In all the XRD patterns of precipitated samples, no peak was observed at low angles ($2\theta = 1$–10°). This suggests the absence of an ordered mesoporous network structure in the as-prepared samples. The as-synthesized TiO_2 powders show broad anatase peaks (see Fig. 3), indicating that they are anatase phase (JCPDS 21-1272). The Scherrer[23] line width analysis of the (101) reflection gives an estimate of the primary crystallite size of the samples TiCTAB10 and TiDCB10 respectively, in the range of 4–5 nm. After heat treatment, only peaks of the anatase phase that become stronger and sharper are identified in all heated samples (see Fig. 3). Average crystalline sizes calculated from the broadening of the (101) XRD peaks of the anatase phase are presented in Table 1 for the samples TiCTAB10_600 and TiDCB10_600 respectively, calcined at temperature 600 °C. The crystalline size decreased with increasing amount of surfactants.

Nitrogen adsorption–desorption isotherms of type IV with a hysteresis loop are typical of mesoporous materials.[24] The pore size distribution of the as-synthesized samples determined by BJH desorption isotherm shows a bimodal pore size distribution consisting of smaller fine ($\sim$2 nm) intra-particle pores and larger ($\sim$5 nm) inter-particle pores. The pore structural parameters of both samples are listed in Table 1. Compared to the reference sample prepared without surfactants (denoted as TIT300), the surface area, pore volume and pore radius increases with the amount of surfactant present during the preparation.

The SEM images of the prepared samples are presented in Fig. 2. The SEM micrographs show roughly spherical particles that are $\sim$2 μm in size, when surfactants were not used. When the concentration of the surfactants in the reaction mixture is increased, the spherical particles are transformed to the mesoporous phase (coral-like structures, see Fig. 2b and c). Three structures are formed on the surface of TiO_2 in the order of increasing CTAB and SDBS concentration respectively, have been attributed to the creation of hemimicelle, admicelle, and micelle structures on the surface. A hemimicelle is described as a patchy bilayer in which the second layer is incomplete. The admicelle can be described as a more complete (or less defective) bilayer structure. At the highest CTAB concentration, true micelles adsorb on the surface.[25]

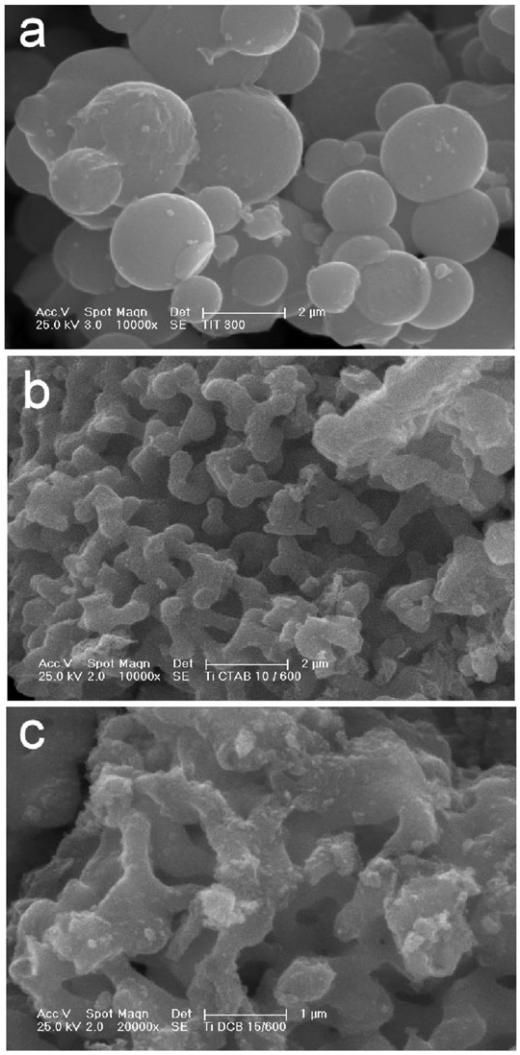

Fig. 2 SEM images of titania: (a) TIT 300 without surfactants, (b) TiCTAB10, (c) TiDCB10.

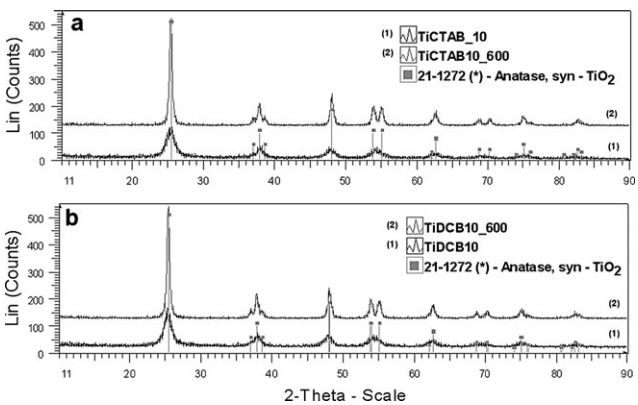

Fig. 3 XRD pattern of the samples: (a) TiCTAB10; (b) TiDCB10.

The micellar structures (see white arrow) created on the TiO_2 surface in the unheated sample named TiCTAB10 are presented in Fig. 4a and b. Fig. 4b shows that the micelles form a wormhole-like pore texture, the diameter of these pores being 2–3 nm.

Table 1 Crystallite size, surface area, porosity and rate constant k of prepared samples

Sample	Crystallite size [nm]	Surface area [$m^2\ g^{-1}$]	Pore volume [$cm^3\ g^{-1}$]	Micropore surface area [$m^2\ g^{-1}$]	Micropore volume [$cm^3\ g^{-1}$]	$k_{acetone}$ [h^{-1}]	k_{butane} [h^{-1}]
TiCTAB10_600	16.1	42.4	0.1520	2.363	0.00081	0.0273	0.0168
TIDCB10_600	13.7	49.4	0.1418	2.550	0.00090	0.0593	0.0628
TIT300	30.2	162.6	0.1495	0.000	0.00000	0.0254	0.0147

Results obtained by high resolution transmission electron microscopy (HRTEM) are shown in Fig. 5. The HRTEM micrographs in Fig. 5a and b characterized the surface morphology of the sample TIT300. At the HRTEM image (Fig. 5b) are clearly visible amorphous domains, which have a negative effect on photocatalytic activity. By contrast, the sample denoted TiDCB_600 (Fig. 5e and f) has the least of these amorphous domains and therefore also has the highest photocatalytic activity. The absence of these amorphous domains is an essential prerequisite for good photocatalytic properties.

Both samples, TiCTAB_10 and TiDCB_10 have an interlayer spacing of 0.352 nm corresponding to the (101) plane of anatase and consist of primary nanocrystals with a perfect crystal structure. The selected area of diffraction patterns confirmed the anatase phase.

The prepared titania samples with surfactants demonstrated higher photocatalytic activity for degradation of Orange 2 in aqueous solution compared to reference samples prepared without surfactants and to the commercial available photocatalyst Degussa P25. The rate constant of sample TICTAB10_600 was 0.3974 min^{-1}, TiDCB_10 was 0.4906 min^{-1} and P25 was 0.1907 min^{-1}.[26] Blank tests (a layer of poly(hydroxyethyl methacrylate) without titania) were performed in order to establish the effect of photolysis and catalysis on the conversion of acetone and n-butane. Non-measurable conversion of the target gases was detected with UV illumination, and no acetone or butane (respectively) were absorbed in the poly(hydroxyethyl methacrylate) matrix. The injection concentration of acetone was 0.4 ml (liquid) and of butane was 100 ml (gas), respectively.

When organic compounds are chemically transformed by a photocatalytic oxidation reaction, it is the hydroxyl radical ($OH^{\bullet}$), derived from the oxidation of adsorbed water or adsorbed $OH^{\bullet}$, that is the dominant strong oxidant. Its net reaction with a volatile organic compound (VOC) can be expressed as:

$$OH^{\bullet} + VOC + O_2 \rightarrow nCO_2 + mH_2O \quad (1)$$

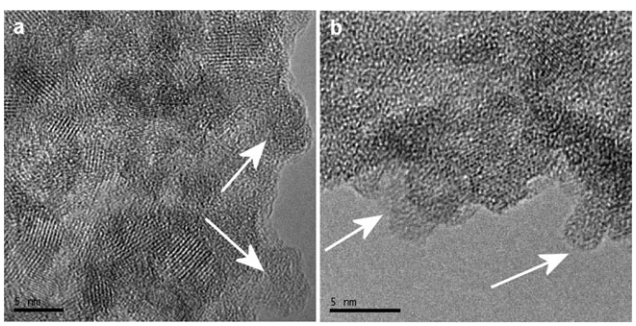

Fig. 4 HRTEM micrograph of unheated sample TiCTAB10: (a) micellar structure, (b) wormhole-like structure.

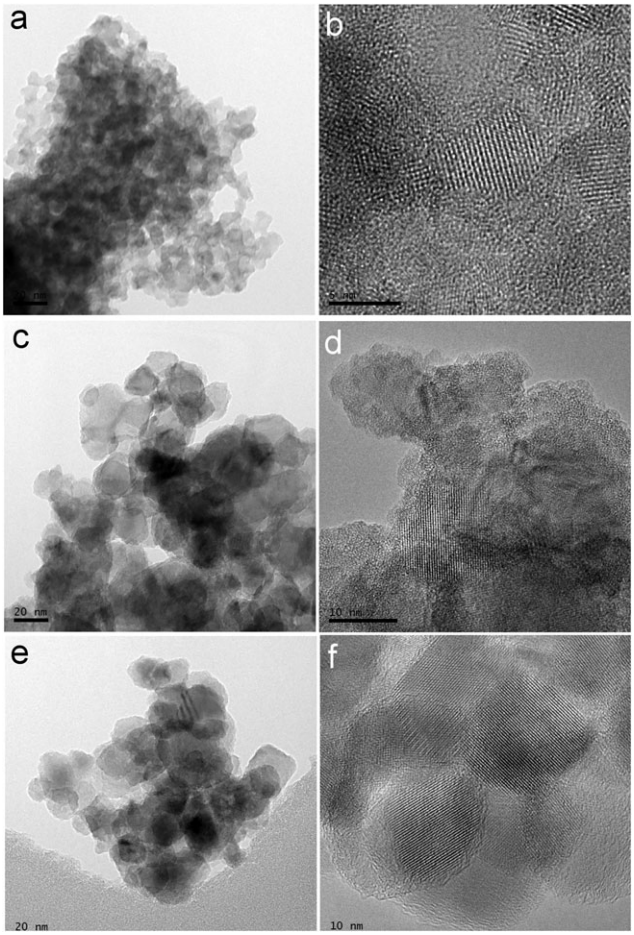

Fig. 5 HRTEM micrograph of sample denoted as: (a–b) TIT300, (c–d) TiCTAB10_600, (e–f) TiDCB10_600.

Acetone (CH_3COCH_3) is a common chemical used extensively in a variety of industrial and domestic applications. Therefore, we chose it as a model contaminant. Photocatalytic oxidation of butane[27] and acetone[28] are based on the following overall reactions:

$$CH_3COCH_3 + 4O_2 \rightarrow 3CO_2 + 3H_2O \quad (2)$$

$$2C_4H_{10} + 13O_2 \rightarrow 8CO_2 + 10H_2O \quad (3)$$

Fig. 6 shows the typical chromatograph of the effluent obtained near butane and acetone photocatalytic oxidation. Only oxygen, carbon monoxide, carbon dioxide, water, butane and acetone were detected at retention times of 1.30, 2.14, 6.27, 9.35 and 10.42 min, respectively. Besides the kinetics of starting components (organic compound and molecular oxygen), time profiles of selected products (carbon dioxide and carbon monoxide) were monitored as well. The corresponding

experimental dependences are plotted in Fig. 7. The rate of degradation was estimated to obey pseudo-first-order kinetics, and hence the rate constant for degradation k was obtained from the first-order plot according to eqn (4), where C_0 is the initial concentration, C is the concentration of acetone or butane after a time (t), and k is the first-order rate constant:

$$\ln(C_0/C) = kt \quad (4)$$

The photocatalytic degradation of butane and acetone respectively, was fitted by theoretical kinetic curves of the first-order kinetics and the corresponding rate constants are given in Table 1. Acetone is a major organic constituent of exhaled human breath and also a typical intermediate photocatalytic oxidation product.[29] The positive holes can oxidize adsorbed water to produce hydroxyl radical. Acetone can react with hydroxyl radical ($OH^{\bullet}$) at the TiO_2 surface to form a dimethyl carbonyl radical ($H_2C^{\bullet}$–CO–CH_3) *via* a metathesis reaction (H-abstraction). This dimethyl carbonyl radical can be decomposed by β-scission with cleavage of C–C bonds in order to produce a methyl radical ($^{\bullet}CH_3$) and ketene ($H_2C{=}C{=}O$).[7] Attwood *et al.*[30] identified an alkylperoxy species, $CH_3COCH_2OO^{\bullet}$, as the intermediate of acetone. The possible pathways are:

$$CH_3COCH_3 + O^{\bullet} \rightarrow CH_3COCH_2^{\bullet} + OH^{\bullet} \quad (5)$$

$$CH_3COCH_2^{\bullet} + O_2 \rightarrow CH_3COCH_2OO^{\bullet} \quad (6)$$

Raillard *et al.*[31] found that the main detected intermediate was acetaldehyde, followed by methyl formate. Thus, the species $CH_3COCH_2OO^{\bullet}$ possibly reacted to form acetaldehyde. The pathway of acetone may be: acetone → acetaldehyde + formic acid or CO_2 → formaldehyde + methanol → formic acid. The generated formic acid and methanol might react to form methyl formate, which was reported by Raillard.[31]

Djeghri *et al.*[32] reported photoinduced oxidation of C_2–C_8 alkanes on TiO_2 at ambient temperature. In general, they observed that alkanes (C_nH_{2n+2}) formed ketones ($C_nH_{2n}O$) and other aldehydes $C_mH_{2m}O$ with $2 < m < n$. If the alkane was branched, the ketone was $C_mH_{2m}O$ with $3 < m < n$. The reactivity of different types of carbon atoms followed the sequence: $C_{tertiary} > C_{quaternary} > C_{secondary} > C_{primary}$. Coronado[6] reports that acetone is adsorbed exclusively in a molecular form on TiO_2. Its photocatalytic oxidation yields acetate and formate complexes, along with adsorbed acetaldehyde and formic acid. These adsorbed molecules can act as intermediates species in the photooxidation of acetone. Fig. 7 shows, that in our case, the reactivity of butane and acetone are different and simpler – no intermediate products such as ketones or aldehydes were detected in the gaseous phase. This means that photocatalytic oxidation proceeds not in the gaseous phase but on the layer surface directly, causing formation of CO, CO_2 and H_2O (water is adsorbed into the layer of poly(hydroxyethyl methacrylate)). This causes total degradation of both butane and acetone after irradiation for about 60 h. At the same time, the photocatalytic activity of two prepared samples of titania photocatalysts named TICTAB and TIDCB were compared, the photocatalyst TIDCB (prepared

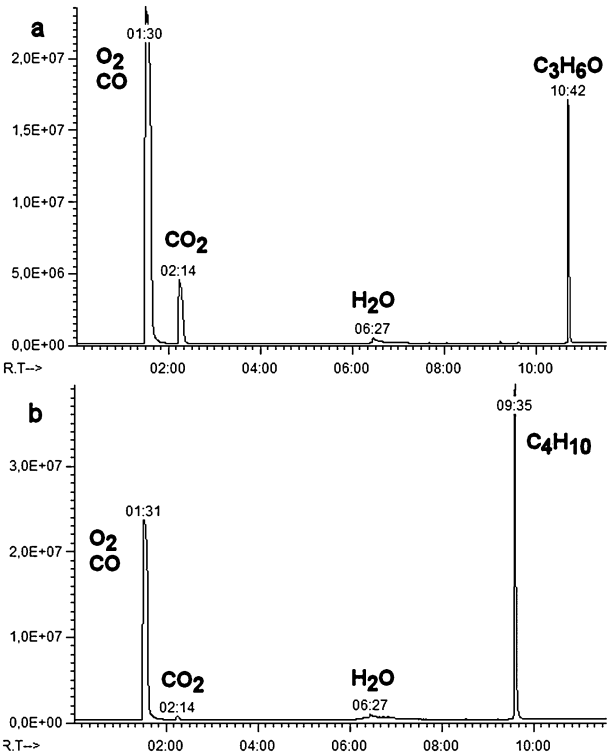

Fig. 6 Gas chromatograph of: (a) acetone, (b) *n*-butane.

with anionic surfactant) showing higher photocatalytic activity. For this purpose, both photocatalysts were first immobilized on glass plates (100 × 150 mm) with poly(hydroxyethyl methacrylate) as bonding agent. The corresponding plate was placed into a home-made batch-mode gas-phase photoreactor (internal volume 3 dm^3) containing a black-light fluorescent tube. Photocatalytic degradation of two model organic substances, acetone and butane, in pure oxygen atmosphere was achieved. From these results, we found that titania prepared with anionic surfactant has a three times better photocatalytic activity then titania prepared with cationic surfactant. At the same time, it was possible to see markedly higher production of CO_2 than of CO (see Fig. 7c and d). The photocatalyst TICTAB (prepared with cationic surfactant) was less photoactive. After 60 h of irradiation, it caused only partial decomposition of both organic compounds (80% of acetone and 65% of butane). At the same time, the concentration of O_2 decayed more slowly, and more CO than CO_2 was produced (see Fig. 7a and b).

It is commonly accepted that mesoporous TiO_2 with a large surface area is a superior photocatalyst, since a larger surface area offers more active adsorption sites. However, it is difficult to explain the high activity of mesoporous TiO_2 based solely on its surface area. According to work,[33] the reaction of acetone on mesoporous titania generally follows a 3/2-order kinetics model:

$$r = kC^{3/2} \quad (7)$$

where r is the surface-based reaction rate, k is the reaction rate constant, and C is the concentration.

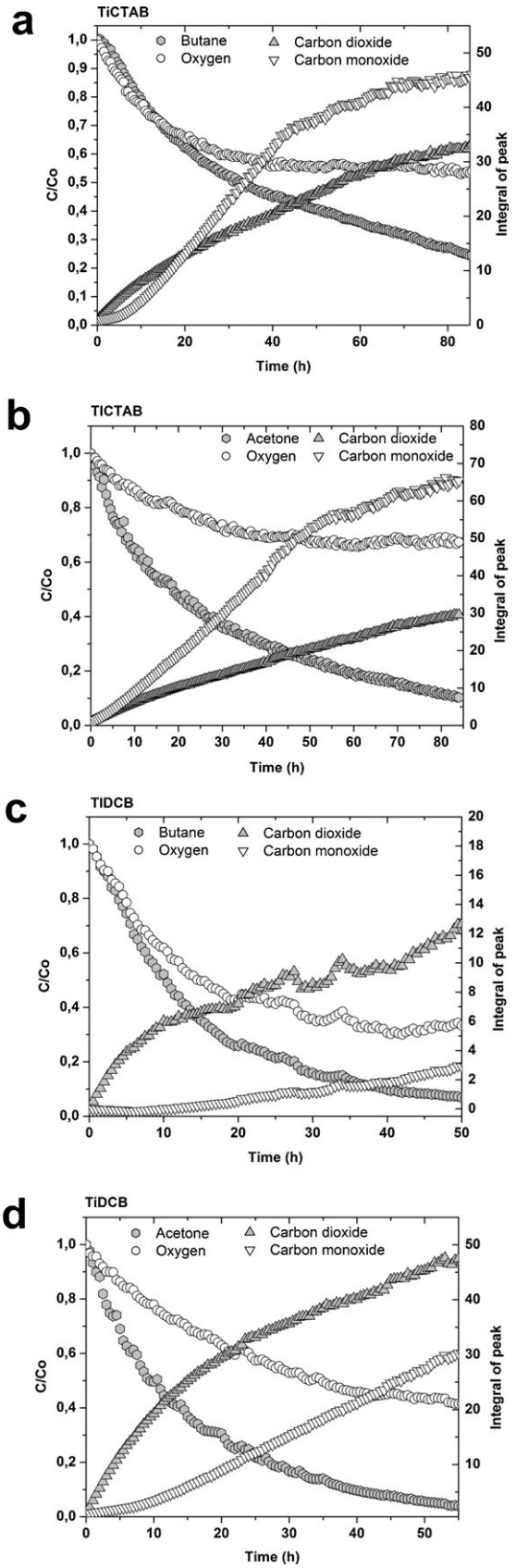

Fig. 7 Kinetics of the photocatalytic degradation of: butane on layers (a) TiCTAB10_600 and (c) TiDCB10_600; and acetone on samples (b) TiCTAB10_600 and (d) TiDCB10_600.

A mass balance can be used in conjunction with this reaction rate model to derive an expression relating reactor space time to conversion:[34]

$$\frac{WS}{A}C^{1/2} = \frac{1}{k}\left(\frac{2}{(1-f)^{1/2}} - 2\right) \qquad (8)$$

where W is the weight of catalyst, V is the inlet volumetric flow, f is the fractional conversion of acetone, and S is the surface area of titania.

According to eqn (8), one would assume that the efficiency of photocatalysis is proportional to the surface area. Experimentally, however, samples annealed at 600 °C are more active. This can be explained by the presence of micro-channels in the mesoporous structure of the photocatalyst. There is good reason to think that micro-channels can cause two positive effects, namely, increasing efficiency and improving mass transfer photoabsorption. In the mesoporous structure of TiO_2, micro-channels can act as channels of light-transfer path propagating the incident photon flux near the inner surface of mesoporous TiO_2. This allows light to penetrate deeper into the catalyst, and therefore the use of light is more effective. Considering light absorption, reflection and scattering within such a mesoporous system, the effective light-active surface is much larger. This improves the photocatalytic efficiency of the catalyst.

Conclusion

Photocatalytic activity of two samples of titania photocatalysts named TICTAB and TIDCB were compared. Both photocatalysts were first immobilized on glass plates (100 × 150 mm) with poly(hydroxyethyl methacrylate) as a bonding agent. The corresponding plate was placed into a home-made batch-mode gas-phase photoreactor (internal volume 3 dm^3) containing a black-light fluorescent tube. Photocatalytic degradation of two model organic substances, acetone and butane, in pure oxygen atmosphere was achieved. Importantly, photocatalytic degradation took place without undesirable intermediate products being produced. This article therefore presents results which, uniquely, stand in contrast to well-known research on the same topic, by confirming that porous structures influence the photocatalytic activity of materials. The greater photocatalytic activity of our specimens appears to have been caused by the mesoporous structure, and titania prepared with an anionic surfactant has three times better photocatalytic activity than titania prepared with a cationic surfactant. The HRTEM images clearly show that sample TiDCB10_600 is a highly crystalline material, which contains no amorphous domains. The absence of these amorphous domains is an essential prerequisite for good photocatalytic properties.

Acknowledgements

This work was supported by the Academy of Sciences of the Czech Republic (Project No. AV OZ 40320502) and Czech Science Foundation (Project No. 203/08/0335).

References

1 V. Collins-Martínez, A. L. Ortiz and A. A. Elguézabal, Influence of the anatase/rutile ratio on the TiO_2 photocatalytic activity for the photodegradation of light hydrocarbons, *Int. J. Chem. Reactor Eng.*, 2007, **5**, A92.

2 T. M. Twesme, D. T. Tompkins, M. A. Anderson and T. W. Root, Photocatalytic oxidation of low molecular weight alkanes: Observations with ZrO_2–TiO_2 supported thin films, *Appl. Catal., B*, 2006, **64**, 153–160.

3 A. Haeger, O. Kleinschmidt and D. Hesse, Kinetics of photocatalyzed gas reactions using titanium dioxide as the catalyst, Part II: Photocatalyzed total oxidation of alkanes with oxygen, *Chem. Eng. Technol.*, 2004, **27**, 9.

4 M. M. Yoshida, V. C. Martínez, P. A. Madrid and A. A. Elguézabal, Thin films of photocatalytic TiO_2 and ZnO deposited inside a tubing by spray pyrolysis, *Thin Solid Films*, 2002, **419**, 60–64.

5 J. Yu, M. Zhou, B. Cheng, H. Yu and X. Zhao, Ultrasonic preparation of mesoporous titanium dioxide nanocrystalline photocatalysts and evaluation of photocatalytic activity, *J. Mol. Catal. A: Chem.*, 2005, **227**, 75–80.

6 J. M. Coronado, S. Kataoka, I. T. Tejedor and M. A. Anderson, Dynamic phenomena during the photocatalytic oxidation of ethanol and acetone over nanocrystalline TiO_2: simultaneous FTIR analysis of gas and surface species, *J. Catal.*, 2003, **219**, 219–230.

7 G. Vincent, P. M. Marquaire and O. Zahraa, Abatement of volatile organic compounds using an annular photocatalytic reactor: Study of gaseous acetone, *J. Photochem. Photobiol., A*, 2008, **197**, 177–189.

8 W. Choi, J. Y. Ko, H. Park and J. S. Chung, Investigation on TiO_2-coated optical fibers for gas-phase photocatalytic oxidation of acetone, *Appl. Catal., B*, 2001, **31**, 209–220.

9 C. Raillard, V. Héquet, P. Le Cloirec and J. Legrand, Kinetic study of ketones photocatalytic oxidation in gas phase using TiO_2-containing paper: effect of water vapor, *J. Photochem. Photobiol., A*, 2004, **163**, 425–431.

10 J. Peral and D. F. Ollis, Heterogeneous photocatalytic oxidation of gas-phase organics for air purification: Acetone, 1-butanol, butyraldehyde, formaldehyde, and *m*-xylene oxidation, *J. Catal.*, 1992, **136**, 554–565.

11 S. H. Kim, S. B. Kim, G. S. Kim, H. T. Jang and S. C. Hong, Kinetic study on degradation of gaseous acetone over thin-film TiO_2 photocatalyst in a continuous flow system, *React. Kinet. Catal. Lett.*, 2007, **90**, 85–91.

12 J. C. Yu, J. Lin and R. W. M. Kwok, $Ti_{1-x}Zr_xO_2$ Solid solutions for the photocatalytic degradation of acetone in air, *J. Phys. Chem. B*, 1998, **102**, 5094–5098.

13 J. C. Yu, J. Lin and R. W. M. Kwok, Enhanced photocatalytic activity of $Ti_{1-x}V_xO_2$ solid solution on the degradation of acetone, *J. Photochem. Photobiol., A*, 1997, **111**, 199–203.

14 M. Addamo, M. Bellardita and A. Di Paola L. Palmisano, Preparation and photoactivity of nanostructured anatase, rutile and brookite TiO_2 thin films, *Chem. Commun.*, 2006, 4943–4945.

15 A. Di Paola, M. Addamo, M. Bellardita, E. Cazzanelli and L. Palmisano, Preparation of photocatalytic brookite thin films, *Thin Solid Films*, 2007, **515**, 3527–3529.

16 *JCPDS PDF-2*, release 2001, ICDD Newtown Square, PA, USA.

17 *ICSD Database*, FIZ Karlsruhe, Germany, 2008.

18 S. Brunauer, P. H. Emmett and E. Teller, Adsorption of Gases in Multimolecular Layers, *J. Am. Chem. Soc.*, 1938, **60**, 309.

19 E. P. Barret, L. G. Joyner and P. P. Halenda, The determination of pore volume and area distributions in porous substances. I. Computations from nitrogen isotherms, *J. Am. Chem. Soc.*, 1951, **73**, 373.

20 G. Soler-Illia, M. Jobbagy, R. J. Candal, A. E. Regazzoni and M. A. Blesa, Synthesis of metal oxide particles from aqueous media: The homogeneous alkalinization method, *J. DispersionSci. Technol.*, 1998, **19**, 207–228.

21 V. Štengl, J. Šubrt, P. Bezdička, M. Maříková and S. Bakardjieva, Homogeneous precipitation with urea—An easy process for making spherical hydrous metal oxides, *Solid State Phenom.*, 2003, **90–91**, 121–126.

22 S. Bakardjieva, J. Šubrt, V. Štengl, M. J. Dianez and M. J. Sayagues, Photoactivity of anatase–rutile TiO_2 nanocrystalline mixtures obtained by heat treatment of homogeneously precipitated anatase, *Appl. Catal., B*, 2005, **58**, 193–202.

23 P. Scherrer, *Gottinger Nachrichte*, 1918, **2**, 98.

24 S. Lowell and J. E. Shields, *Powder Surface Area and Porosity*, Chapman & Hall, 1998.

25 H. Li and C. P. Tripp, Use of Infrared Bands of the surfactant headgroup to identify mixed surfactant structures adsorbed on titania, *J. Phys. Chem. B*, 2004, **108**, 18318–18326.

26 V. Houškova, V. Štengl, S. Bakardjieva and N. Murafa, Synthesis of mesoporous titania by homogeneous hydrolysis of titania oxo-sulfate in the presence of cationic and anionic surfactants, in press.

27 M. J. Lorences, G. S. Patience, F. V. Díez and J. Coca, Transient n-butane partial oxidation kinetics over VPO, *Appl. Catal., A*, 2004, **263**, 193–202.

28 H. Yu, J. Yu and B. Cheng, Photocatalytic activity of the calcined H-titanate nanowires for photocatalytic oxidation of acetone in air, *Chemosphere*, 2007, **66**, 2050–2057.

29 A. Wisthaler, P. Strom-Tejsen, L. Fang, T. J. Arnaud, A. Hansel, T. D. Mark and D. P. Wyon, PTR-MS assessment of photocatalytic and sorption-based purification of recirculated cabin air during simulated 7-h flights with high passenger density, *Environ. Sci. Technol.*, 2007, **41**, 229–234.

30 A. L. Attwood, J. L. Edwards, C. C. Rowlands and D. M. Murphy, Identification of a surface alkylperoxy radical in the photocatalytic oxidation of acetone/O-2 over TiO_2, *J. Phys. Chem. A*, 2003, **107**, 1779–1782.

31 C. Raillard, V. Hequet, P. Le Cioirec and J. Legrand, Photocatalytic oxidation of ethyl ketone over sol–gel and commercial TiO_2 for the improvement of indoor air, *Water Sci. Technol.*, 2006, **53**, 107–115.

32 N. Djeghri, M. Formenti, F. Juillet and S. J. Teichner, Photointeraction on the surface of titanium dioxide between oxygen and alkanes, *Faraday Discuss. Chem. Soc.*, 1974, **58**, 185–193.

33 M. E. Zorn, D. T. Tompkins, W. A. Zeltner and M. A. Anderson, Photocatalytic oxidation of acetone vapor on TiO_2/ZrO_2 thin films, *Appl. Catal., B*, 1999, **23**, 1–8.

34 X. Wang, J. C. Yu, C. Ho, Y. Hou and X. Fu, Photocatalytic activity of a hierarchically macro/mesoporous titania, *Langmuir*, 2005, **21**, 2552–2559.